Optimal Shape Design of Pressure-Driven Curved Micro Channels with Hydrophilic and Hydrophobic Walls

Seokhyun Lim* and Haecheon Choi**

* School of Mechanical and Aerospace Engineering, Seoul National University, Seoul 151-744, Korea, limsh@stokes.snu.ac.kr
** School of Mechanical and Aerospace Engineering, Seoul National University, Seoul 151-744, Korea, choi@socrates.snu.ac.kr

ABSTRACT

In this study, we perform an optimal shape design of a pressure-driven curved micro channel with minimum pressure drop using a mathematical theory. We consider two different wall types such as hydrophobic and hydrophilic walls where the slip and no-slip conditions are applied, respectively. Optimal shapes are obtained from the initial circular shapes, which are commonly used in most curved channels, at three different bulk Reynolds numbers of 0.1, 1 and 10 for both the 90° and 180° curved channels. In the optimal shape, the height of the curved channel is widened according to the optimality condition, and the pressure drop is significantly reduced by about 10% ~ 20% as compared to that with the initial circular shape.

Keywords: curved micro channel, pressure drop, optimal shape design, hydrophilic wall, hydrophobic wall.

1 INTRODUCTION

Flow in a microchannel is driven by the difference between the pressures at the inlet and exit or between the electric potentials. For the first case (pressure-driven flow), an important issue is how to reduce the pressure drop required to drive a constant mass flow rate in a channel. In microfluidic applications such as LOC, 90° and 180° curved channels are frequently used to supply long flow passage in a compact volume. In most curved channels, the part connecting two straight channels is made of circular walls. However, modification of the shape in the connection part may significantly reduce the pressure loss.

For the pressure-driven liquid flow in a micro channel, the no-slip boundary condition is not always valid. That is, fluids do not slip at the hydrophilic micro channel wall but do slip at the hydrophobic wall [1, 2]. The slip velocity for the hydrophobic wall can be described by the well-known Navier's hypothesis, $u|_w = \alpha \cdot \partial u/\partial n|_w$, where $u|_w$ is the slip velocity at the wall, $\partial u/\partial n|_w$ is the wall-normal velocity gradient at the wall, and α is the slip length. The fluid slip at the hydrophobic wall results in the reduction of the skin friction (or the reduction of the pressure drop) as compared to the case of the hydrophilic wall [3].

Therefore, we design the optimal shapes of pressure-driven curved micro channels with the hydrophobic and hydrophilic walls, respectively, in this study. The optimal shapes are obtained using an optimal control theory based on the variational calculus and the gradient algorithm [4, 5] at three different bulk Reynolds numbers of 0.1, 1 and 10 for both the 90° and 180° curved channels.

2 SHAPE DESIGN ALGORITHM

Figure 1 shows the schematic diagram of a two dimensional 90° circular-shaped curved micro channel. Inner and outer radii of the circular channel are R_I and R_O, and the streamwise lengths of the inlet and outlet channels are L_1 and L_2, respectively. Γ_M represents the wall boundary of the circular channel to be designed, Γ_I and Γ_O are the channel entrance and exit boundaries, and Γ_F represents the fixed wall boundaries of the two straight inlet and outlet channels. Γ_M, Γ_I, Γ_O and Γ_F constitute Γ and the inner domain enclosed by Γ is Ω. P_ϵ in figure 1 is determined by moving each point P on Γ_M in outward normal direction by the magnitude of $\epsilon\zeta(s)$, where $\zeta(s)$ is an arbitrary function of the arc length s. $\Gamma_{M,\epsilon}$ is a new curved channel wall that consists of $P'_\epsilon s$. Here ϵ is a very small positive number.

The flow inside the curved channel is assumed to be steady, incompressible laminar and satisfies the continuity and Navier-Stokes equations:

$$\begin{aligned} u_{i,i} &= 0, \\ \rho u_j u_{i,j} &= -p_{,i} + \mu u_{i,jj}, \end{aligned} \tag{1}$$

where u_i are the velocities, ρ the density, p the pressure and μ the viscosity. Flow at the entrance of the micro channel is a fully developed laminar channel flow and flow at the exit is assumed to be fully developed with a sufficiently long outlet channel. The no-slip and slip boundary conditions are applied to the hydrophilic and hydrophobic walls, respectively:

$$\begin{cases} u_i = 0 & \text{at hydrophilic wall,} \\ u_n = 0 \;\&\; u_s = \alpha \dfrac{\partial u_s}{\partial n} & \text{at hydrophobic wall,} \end{cases} \tag{2}$$

where u_n and u_s are the wall-normal and tangential velocities at wall, respectively. The Reynolds number is

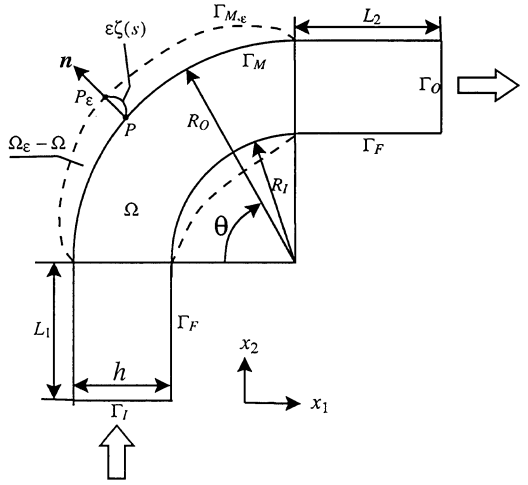

Figure 1: Schematic diagram of a curved micro channel.

defined as $Re = u_m h/\nu = u_m(R_O - R_I)/\nu$, where u_m is the bulk mean velocity at the channel entrance and h is the channel height.

In this study, we are to obtain the optimal shape of Γ_M to minimize the driving force or the pressure difference between the channel exit and entrance. Therefore, the cost function maximized is defined as

$$J(\Gamma_M) = \int_{\Gamma_I} pu_i n_i ds + \int_{\Gamma_O} pu_i n_i ds, \qquad (3)$$

where n_i is the outward normal unit vector.

Let δJ be the variation of the cost function due to the shape change of the curved channel wall from Γ_M to $\Gamma_{M,\epsilon}$, and it can be determined using the variational calculus as (the detailed procedure is not shown in this paper)

$$\delta J = \mu \int_{\Gamma_M} \zeta(s) \left(\frac{\partial u_s}{\partial n} - \alpha \cdot \frac{\partial^2 u_s}{\partial n^2} \right) \frac{\partial z_s}{\partial n} ds, \qquad (4)$$

where u_s and z_s are the velocity and adjoint velocity, respectively, in the tangential direction. Equation (4) represents the variation of the cost function for both cases of the hydrophilic ($\alpha = 0$) and hydrophobic ($\alpha \neq 0$) walls. Here, z_i and q are the adjoint velocity and pressure that satisfy the following adjoint equations:

$$\begin{aligned} z_{i,i} &= 0, \\ \mu z_{i,jj} + \rho u_j (z_{i,j} + z_{j,i}) - q_{,i} &= 0. \end{aligned} \qquad (5)$$

The wall boundary conditions for the adjoint velocity are similar to those of the velocity:

$$\begin{cases} z_i = 0 & \text{at hydrophilic wall,} \\ z_n = 0 \;\&\; z_s = \alpha \dfrac{\partial z_s}{\partial n} & \text{at hydrophobic wall.} \end{cases} \qquad (6)$$

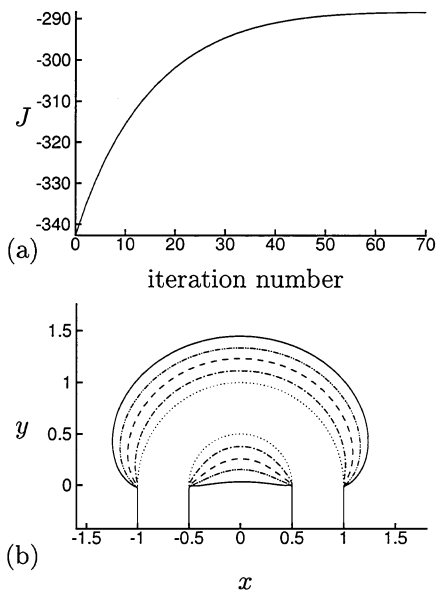

Figure 2: Variations of (a) the cost function and (b) shape at successive iterations (Re=1): ·····, iteration=0; -·-·-, 15; – – –, 30; -···-, 45; ———, 60.

Here, when we define $\zeta(s)$ as

$$\zeta(s) = \omega(s) \left(\frac{\partial u_s}{\partial n} - \alpha \cdot \frac{\partial^2 u_s}{\partial n^2} \right) \frac{\partial z_s}{\partial n}, \qquad (7)$$

δJ is always positive, where $\omega(s)$ is a nonnegative weighting function. Therefore, a new shape obtained by moving the wall boundary by $\epsilon\zeta(s)$ guarantees the increase of the cost function J. From (7), it is clear that the optimality condition for minimum pressure drop is zero skin friction at the curved hydrophilic wall, whereas at the curved hydrophobic wall it becomes $\partial u_s/\partial n - \alpha \cdot \partial^2 u_s/\partial n^2 = 0$.

From the initial circular-shaped curved channel, we iterate the shape until the cost function converges to its maximum. For the shape design of a 180° curved micro channel, the optimality condition and design procedure are the same as those for 90° curved one.

Steady, incompressible Navier-Stokes and adjoint equations are solved using the SIMPLER algorithm [6]. The convective terms in the Navier-Stokes equations are discretized using the third-order QUICK scheme [7].

The lengths of the two straight inlet and outlet channels are $L_1 = 3$ and $L_2 = 6$, and the inner and outer radii of the initial circular-shaped curved channel are $R_I = 0.5$ and $R_O = 1$, and the height of the straight channel is $h = R_O - R_I = 0.5$. With each change of the shape, the grids are generated automatically using an elliptic/hyperbolic hybrid grid generation program. The numbers of grid points are 256×64 and 288×64 for

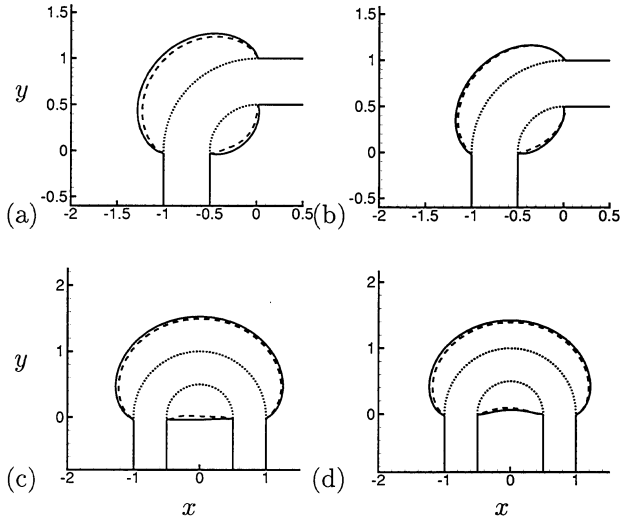

Figure 3: Optimal shapes of 90° and 180° curved channels: (a), (c) hydrophilic wall; (b), (d) hydrophobic wall. ·····, Initial shape; ———, Re=0.1; -·-·-·-, Re=1; – – – –, Re=10.

the 90° and 180° curved channels, respectively. The optimal shapes of the curved micro channels are obtained for both the hydrophilic and hydrophobic walls at three different bulk Reynolds numbers of 0.1, 1 and 10. The velocity boundary conditions at the hydrophobic wall are given in (2) with $\alpha = 0.05$.

3 RESULTS

Figure 2 shows the variations of the cost function and shape at successive iterations for the 180° curved micro channel with the hydrophobic wall at $Re = 1$. As the iteration number increases, the cost function increases and converges to its maximum. The height of the curved channel is widened and the shape of the channel is significantly modified. When the iteration number is larger than 40, the cost function increases very little but the shape keeps changing. At the iteration numbers of 15, 30, 45 and 60, the corresponding reductions in the pressure drop are 10.6 %, 14.2 %, 15.4 % and 15.8 %, respectively, as compared with that of the initial circular shape. Inspite of the non-negligible difference in the shapes at the iteration numbers of 45 and 60, the reductions in the pressure drop are nearly the same, indicating that no further change in the shape is required. The same tendencies are observed in all cases of 90° and 180° curved channels with the hydrophobic and hydrophilic walls at $Re = 0.1$, 1 and 10.

Figure 3 shows the optimal shapes of 90° and 180° curved channels at various Reynolds numbers. The optimal shapes shown in this figure are obtained with the same convergence criteria such that the increase in the

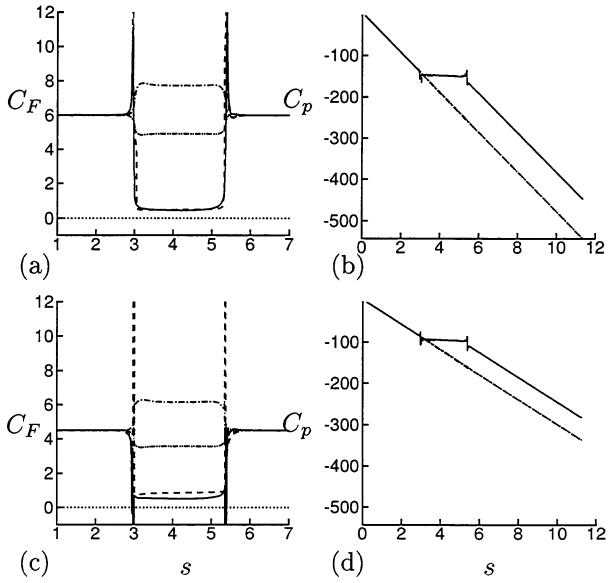

Figure 4: Distributions of C_F and C_p along the inner and outer walls of the 180° curved channel at Re=1: (a), (b) hydrophilic wall; (c), (d) hydrophobic wall. -·-·-·-, Along the inner wall of the initial shape; -·····-, along the outer wall of the initial shape; – – – –, along the inner wall of the optimal shape; ———, along the outer wall of the optimal shape.

cost function per iteration is less than 0.1 % of the total increase in the cost function. Apparently, the heights of the optimal curved channels with the hydrophobic wall are smaller than those with the hydrophilic wall, and the height becomes slighty smaller with increasing Reynolds number. However, it should be mentioned that Fig. 3 does not precisely show the dependence of the optimal shape on the Reynolds number and the wall type, because the pressure drop becomes very insensitive to the shape change near the optimal shape.

Figure 4 shows the distributions of the skin-friction coefficient, $C_F \equiv (\partial u/\partial n - \alpha \partial^2 u/\partial n^2)/(u_m/h)$, and the pressure coefficient, $C_p \equiv (p - p_I)/(\rho u_m^2/2)$, along the inner and outer walls of the 180° curved channel at Re=1, where s is the arc length along the centerline of the channel from the entrance of the straight inlet channel. In figure 4, $0 \leq s < 3$ corresponds to the straight inlet channel region, $3 \leq s < 5.36$ the curved wall region, and $5.36 \leq s < 11.36$ the straight outlet channel region. In the optimal shape, the value of C_F is nearly (although not exactly) zero along the inner and outer walls, and the pressure is nearly constant in the curved wall region. With the optimal shape, the pressure drop is significantly reduced by about 10% $\sim$ 20% as compared to that with the initial shape.

In figure 5, we show the pressure distributions inside

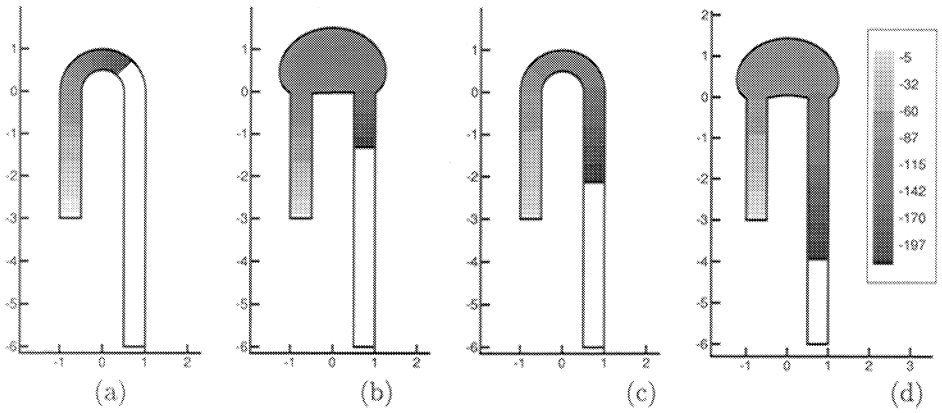

Figure 5: Pressure distribution inside 180° curved channels at Re=1: (a) initial shape with the hydrophilic wall; (b) optimal shape with the hydrophilic wall; (c) initial shape with the hydrophobic wall; (d) optimal shape with the hydrophobic wall.

the initial and optimal shapes of 180° curved channels at Re=1. From this figure, it is clear that with the optimal shape fluids can be driven further downstream. Therefore, one may use a micro pump with a smaller power by modifying the shape of the curved channel and thus micro system becomes much smaller.

4 CONCLUSIONS

In the present study, we designed the optimal shapes of 90° and 180° curved micro channels with minimum driving force using a mathematical theory at three different bulk Reynolds numbers of 0.1, 1 and 10. Two different wall types of hydrophilic and hydrophobic walls were considered. The slip boundary condition that may be described by the Navier's hypothesis was applied for the hydrophobic wall, while the no-slip boundary condition for the hydrophilic wall. The optimal shapes were obtained iteratively based on the gradient method from the initial circular shape. We iterated the curved channel wall shape until the cost function did not increase within a given convergence criteria. In the optimal shape, the height of the curved channel was widened according to the optimality condition. With the optimal shape, the pressure drop was significantly reduced by about $10\% \sim 20\%$ as compared to that with the initial shape.

This work is supported by the Creative Research Initiatives of the Korean Ministry of Science and Technology.

REFERENCES

[1] P. A. Thompson and S. M. Troian, "A General Boundary Condition for Liquid Flow at Solid Surfaces," Nature, vol. 389, no. 25, 360-362, 1997.

[2] D. C. Tretheway and C. D. Meinhart,"Apparent Fluid Slip at Hydrophobic Microchannel Walls," Physics of Fluids, vol. 14, no. 3, L9-L12, 2002.

[3] K. Watanabe, Yanuar and H. Udagawa, "Drag Reduction of Newtonian Fluid in a Circular Pipe with a Highly Water-Repellent Wall," J. Fluid Mech., vol. 381, 225-238, 1999.

[4] O. Pironneau, "On Optimum Design in Fluid Mechanics," J. Fluid Mech., vol. 64, 97-110, 1974.

[5] H. Cabuk and V. Modi, "Optimum Plane Diffusers in Laminar Flow," J. Fluid Mech., vol. 237, 373-393, 1992.

[6] S. V. Patankar, "Numerical Heat Transfer and Fluid Flow," McGraw-Hill, 1980.

[7] B. P. Leonard, "A Stable and Accurate Convective Modelling Procedure Based on Quadratic Upstream Interpolation," Computer Methods in Applied Mechanics and Engineering, vol. 19, 59-98, 1979.